

# Effect of preparation conditions on the physical and hydrophobic properties of two step processed ambient pressure dried silica aerogels

A. PARVATHY RAO

*Air Glass Laboratory, Physics Department, Shivaji University, Kolhapur-416004, Maharashtra, India*

G. M. PAJONK

*LACE-ISM, UMR CNRS Universite Claude Bernard Lyon, 43 bd du 11 Novembre 1918, 69622, Villeurbanne Cedex, France*

A. V. RAO\*

*Air Glass Laboratory, Physics Department, Shivaji University, Kolhapur-416004, Maharashtra, India*

*E-mail: avrao\_phy@unishivaji.ac.in; raouniv@yahoo.com*

The experimental results on the physical and hydrophobic properties of the ambient pressure dried silica aerogels as a function of sol-gel and drying conditions, are reported. The aerogels have been produced by a two stage (acidic and basic) catalytic sol-gel process using tetraethylorthosilicate (TEOS) precursor, oxalic acid (OXA) and ammonium hydroxide (NH<sub>4</sub>OH) catalysts, ethanol (EtOH) solvent and hexamethyldisilazane (HMDZ) silylating agent at 200°C. The molar ratios of HMDZ/TEOS (M), OXA/TEOS (A) NH<sub>4</sub>OH/TEOS (B), acidic H<sub>2</sub>O/TEOS (Wa) basic H<sub>2</sub>O/TEOS (Wb), EtOH/TEOS (S) were varied from 0.09 to 0.9,  $3.115 \times 10^{-5}$  to  $3.115 \times 10^{-3}$ ,  $4 \times 10^{-3}$  to  $8 \times 10^{-2}$ , 2 to 9, 1.25 to 5 and 1 to 16 respectively. The physical properties such as the percentage (%) of volume shrinkage, density, thermal conductivity, percentage of porosity, the percentage of optical transmission and contact angle have been found to be strongly dependent on the sol-gel parameters. It was found from the FTIR spectra of the aerogels that with the increase of M, the bands at 3500 and 1600 cm<sup>-1</sup> corresponding to H-OH and Si-OH respectively decreased and the bands at 840 and 1250 cm<sup>-1</sup> due to Si-C and 2900 and 1450 cm<sup>-1</sup> due to C-H increased. The best quality silica aerogels in terms of low density, low volume shrinkage, low thermal conductivity, high hydrophobicity and high optical transmission have been obtained with the molar ratio of TEOS:EtOH:acidicH<sub>2</sub>O:basicH<sub>2</sub>O:OXA:NH<sub>4</sub>OH:HMDZ at 1:8:3.75:2.25:6.23 × 10<sup>-5</sup>: 4 × 10<sup>-2</sup>:0.36 respectively, by ambient pressure dried method.

© 2005 Springer Science + Business Media, Inc.

## 1. Introduction

Aerogels with water contact angle higher than 150° i.e., with superhydrophobic surfaces and hence low surface energy, are of great interest for various applications such as frictionless flow of liquids, microfluidic devices and corrosive resistant coatings on stainless steel and metals [1, 2]. Silica aerogels have become quite popular because of their special and unusual properties such as high surface area (~1000 m<sup>2</sup>/g), low density (~0.030 gm/cm<sup>3</sup>), high optical transmission (~90%), high porosity (~99%), low thermal conductivity (~0.020 W/mK) and low dielectric constant (~2) [3–7]. Therefore, they have a number of applications such as shock wave studies at high pressures [8], Cerenkov radiation detectors in high energy physics

[9], inertial confinement fusion (ICF) [10], radioluminescent devices [11], containers for liquid rocket propellants [12], micrometeorites [13], light weight thermal and acoustic insulating systems [14], adsorption and catalytic supports [15, 16] and for super capacitors [17, 18]. However, the commercial viability of these materials has been limited mainly by the high cost of supercritical drying.

By varying the sol-gel parameters and pore fluid of wet gel, microstructure of the aerogels may be altered [19]. In the supercritical drying production of the aerogels, the process involves heating and evacuation of highly flammable solvents such as alcohols, which is a risky process at high temperature and pressures. Hence, there is a need to produce silica aerogels by drying

\* Author to whom all correspondence should be addressed.

wet gels at atmospheric pressures. In the year 1995 Prakash et al., reported the synthesis of silica aerogel films at atmospheric pressure using silylation of wet silica gel [20, 21]. Ambient pressure dried aerogels were prepared by chemical modification of silica gels. The hydrophobic nature of the ambient pressure dried aerogels give the structure stability against humidity. Microstructure of the ambient pressure dried aerogels show strikingly similarities with aerogels prepared by supercritical drying.

Aerogels produced using TEOS precursor, in the presence of a strong acid catalyst such as HCl, involves disadvantages such as large gelation time of greater than 3 days, higher volume shrinkage ( $\approx 40\%$ ), low optical transmission ( $\approx 45\%$ ) and higher densities ( $\approx 0.2 \text{ gm/cm}^3$ ) [22]. A few results on acid-base (HCl and  $\text{NH}_4\text{OH}$ ) catalysed aerogels using two step process [23, 24], were reported. However, the aerogels produced using strong acidic catalysts corrode the ovens used for the atmospheric pressure drying. So far, there are no detailed reports on the oxalic acid and ammonium hydroxide two step processed TEOS based silica aerogels by the ambient pressure drying method.

The purpose of using the oxalic acid in the first step and ammonium hydroxide in the second step for the preparation of the aerogels, is for setting the gels in a reasonable amount of time of around one hour. In the case of hydrolysis (acidic) reaction, even though various acids have been used, it has been found that oxalic acid is the best catalyst in terms of lower gelation and the noncorrosive nature. After the acid catalysed reaction, ammonium hydroxide base catalyst is used for the condensation reaction. Ammonium hydroxide is a novel base catalyst because it gets vaporized at the drying temperatures ( $200^\circ\text{C}$ ). We have carried out systematic experimental investigations to obtain the aerogels, with improved properties in terms of low density, high hydrophobicity, low thermal conductivity, high porosity and high optical transmission, by the two step pre-processing using oxalic acid and ammonium hydroxide catalysts at ambient pressure with TEOS precursor and HMDZ silylating agent.

## 2. Experimental

Hydrophobic silica aerogels were produced by the two step acid/base catalysis with HMDZ silylating agent at ambient pressure, as shown in a general scheme of Fig. 1. In the first step, TEOS and ethanol from Fluka Company (puram grade) and oxalic acid (from Merck Company) in water were mixed in the molar ratio of  $1:8:6.23 \times 10^{-5}:3.75$  and stirred at room temperature for 15 min. This mixture was kept for 24 h at room temperature. In the second step, a mixture of  $\text{H}_2\text{O}$  and  $\text{NH}_4\text{OH}$  in the molar ratio of  $2.25:4 \times 10^{-2}$  was added to the silica sol (prepared in the first step) while stirring for 5 min and covered tightly and kept for gelation in 100 ml beakers. After gelation ( $<30 \text{ min}$ ), the beakers containing the gels, were covered with aluminium foils and kept in the PID controlled oven at  $50^\circ\text{C}$  for 3 h to strengthen the gel. The solvent of the gel was exchanged

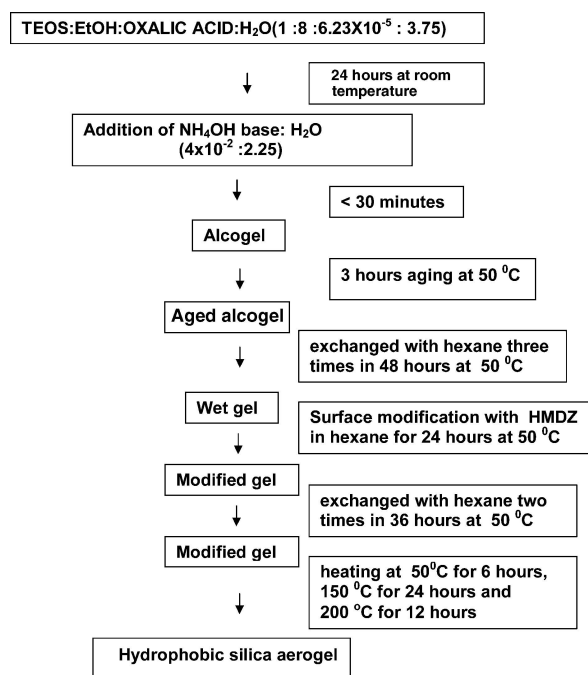


Figure 1 General scheme for the preparation of the two step hydrophobic silica aerogels by ambient pressure dried method.

with hexane 3 times in 48 h. Then the silylation was carried out by immersing the gels in 2–20% HMDZ (0.09 to 0.9 of HMDZ/TEOS molar ratio) in hexane for 24 h at  $50^\circ\text{C}$ . After the silylation process, the solvent exchange was carried out with hexane for two times in 36 h in order to remove the unreacted HMDZ. Finally, the hexane solvent was decanted and pinholes were put in the aluminium foil to control the evaporation and the gels were kept at  $50^\circ\text{C}$  for 6 h,  $150^\circ\text{C}$  for 24 h and  $200^\circ\text{C}$  for 12 h. The oven was switched off and the resulting aerogels were taken out after reaching to the room temperature and used for characterization studies.

### 2.1. Characterization

The bulk density ( $\rho_b$ ) of the aerogels was measured using a known volume of the aerogel and its weight (measured with micro balance,  $10^{-5} \text{ g}$  accuracy), the percentage of volume shrinkage ( $\%V_s$ ) was determined from the change in the volume of the alcogel to the aerogel, using the formula

$$\%V_s = (1 - V_a/V_g) \times 100 \quad (1)$$

where  $V_a$  and  $V_g$  are the volumes of the aerogel and alcogel respectively.

The percentage of porosities and pore volumes of the aerogels were calculated from the equations

$$\text{Percentage of porosity} = [1 - \rho_b/\rho_s] \times 100 \quad (2)$$

and

$$\text{Pore volume} = [1/\rho_b - 1/\rho_s] \quad (3)$$



### 3.1. Drying

The percentage of volume change and the weight loss of the gel during the drying process for the molar ratio of TEOS:EtOH:acidicH<sub>2</sub>O:basic H<sub>2</sub>O:OXA:NH<sub>4</sub>OH:HMDZ at 1:8:3.75:2.25:6.23 × 10<sup>-5</sup>:4 × 10<sup>-2</sup>:0.36, are shown in Fig. 2. It has been found that the percentage of volume change decreased upto 100°C and then increased above 100°C and finally remained constant above 150°C, clearly indicating the spring back effect. At the same time, the percentage of weight loss of the aerogel decreased with increased temperature upto 200°C which is due to the evaporation of the solvent from the gel. During the drying process, in the wet gel, condensation occurs continuously. The capillary force results from the pore fluid evaporation. In non modified gels, drying promotes shrinkage and additional condensation between -OH groups leads to Si—O—Si bond formation and hence making the shrinkage irreversible. Therefore an additional condensation in the wet gel can be prevented by attaching nonreactive -CH<sub>3</sub> species by means of surface modification with silane compounds such as HMDZ. Substitution of -Si-CH<sub>3</sub> for -H also contributes to the gel porosity. The extent of shrinkage of the gel during drying is governed by the capillary pressure (Pr) of the pore fluid [25],

$$Pr = -2\gamma_{LV} \cos \theta / r_p - \delta_t \quad (8)$$

$\gamma_{LV}$  is the liquid/vapour surface tension,  $r_p$  is the radius of the pore,  $\theta$  is the contact angle of the liquid with the wall of the pore and  $\delta_t$  is the thickness of the surface adsorbed liquid layer. The negative sign is due to the negative radius of curvature of the meniscus. Shrinkage occurs until capillary pressure is resisted by the modulus of the solid network [26]. The extent of gel shrinkage is dependent on many factors such as pore size changes during drying and pore size distribution. The modulus of the gel changes dramatically during shrinkage, the gel expands after the critical point and chemical reactions continue during drying which may strengthen the gel. The bulk modulus of the silica network ( $K_p$ ) is given by a power law [27, 28],

$$K_p = K_o(\rho_b/\rho_t)^m \quad (9)$$

where  $\rho_b$  is the bulk density of the network,  $\rho_t$  is the threshold density beyond which the modulus increases in power law, and  $m \approx 3$ .  $K_o$  is the bulk modulus of the silica network when  $\rho_o \leq \rho_t$ . The determination of  $m$  and  $K_o$  was described by Scherer and co-workers [29]. Irreversible shrinkage is due to the fact that the surface of the wet gels are terminated with either hydroxyl (OH) or alkoxy (OR) groups. During the drying these surface groups can react to form =Si—O—Si= bonds via the water or alcohol producing condensation reactions [30] as shown in the Equations 5 and 6. A reversible shrinkage also occurs for non-modifying wet gels if the gels are stiff enough so they are not forced beyond the yield point by the capillary pressure during drying [31]. In the case of effective surface modification, a complete recovery of the volume occurs during the last stage of drying due to the “spring back effect” and similar densi-

ties were obtained as in the case of supercritical drying method.

### 3.2. HMDZ/TEOS molar ratio (M)

The effect of HMDZ on the physical properties of the aerogels, was studied by varying the molar ratio of HMDZ/TEOS ( $M$ ) from 0.09 to 0.9 by keeping the molar ratio of TEOS:EtOH:acidicH<sub>2</sub>O:basicH<sub>2</sub>O:OXA:NH<sub>4</sub>OH constant at 1:8:3.75:2.25:6.23 × 10<sup>-5</sup>:4 × 10<sup>-2</sup> respectively. The % of volume shrinkage and density of the aerogels decreased with increase of the  $M$  from 0.09 to 0.27 and then increased for  $M > 0.36$  as shown in Fig. 3. The density is higher ( $> 0.105$  gm/cm<sup>3</sup>) at lower  $M$  ( $< 0.18$ ) because of incomplete silylation due to less amount of HMDZ and hence the condensation of OH groups leads the gels shrink more during drying. With the increase of  $M > 0.18$ , complete surface modification of the wet gels gives rise to the “spring back effect” and hence shrinkage of the gels is negligible, leading to low density aerogels. Low density ( $\leq 0.09$  gm/cm<sup>3</sup>) aerogels were obtained for  $M$  values in between 0.18 and 0.36.

The porosity of the aerogels increased with an increase of  $M$  up to 0.36 and then it decreased for  $M > 0.36$ . The high porosity silica aerogels were obtained for the  $M$  value of 0.36, even though the % of volume shrinkage for the 0.27 and 0.36 is similar as shown in Figs 3 and 4, because with the addition of more HMDZ, the network structure of the silica gel increased leading to more porosity. The thermal conductivity decreased up to  $M \approx 0.36$  and then increased as shown in Fig. 4. The thermal conductivity depends on the porosity of the aerogels, higher the porosity lesser the thermal conductivity, which is due to less solid content per unit area. In addition, the pore size and the pore size distribution also play a significant role in thermal performance.

The % of optical transmission of the aerogels increased up to an  $M$  value of 0.4 and then decreased for  $M > 0.4$  as shown in Fig. 5. At higher  $M$  ( $> 0.4$ ), more and more -O-Si-(CH<sub>3</sub>)<sub>3</sub> groups were attached to the already formed silica clusters resulting in less cross linking between clusters and leading to change in the particle and pore sizes. Optical properties of the

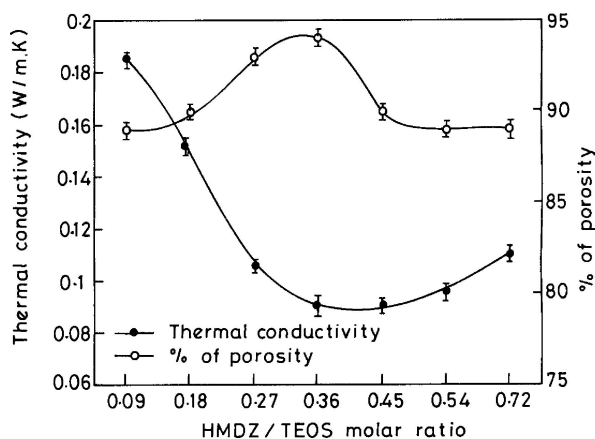


Figure 4 Change in the thermal conductivity and % of porosity of the aerogels with the variation of the HMDZ/TEOS ( $M$ ) molar ratio.

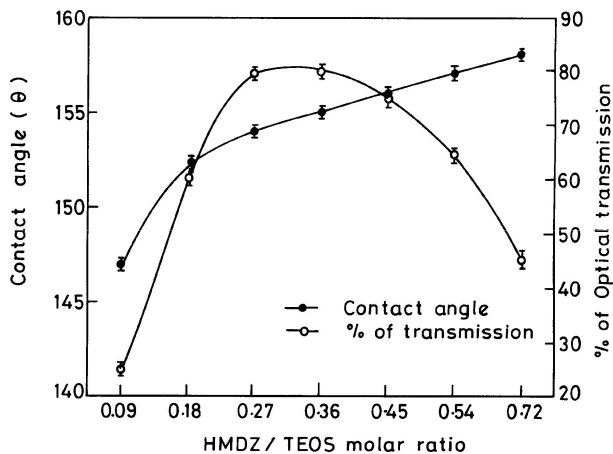


Figure 5 Change in the contact angle and % of optical transmission of the aerogels with the variation of the HMDZ/TEOS ( $M$ ) molar ratio.

aerogels are largely dependent on the pore and particle sizes and their distributions and particle density. Optical clarity is governed by the light scattering results through inhomogeneities between the air and the solid matrix of the aerogel. Although typical length scale within aerogel pore structures and the primary  $\text{SiO}_2$  building blocks is far below (10–70 nm) the wavelength of visible range (400–700 nm), even just a small fraction of large pores and particles are enough to enhance the scattering, therefore at high  $M$  (0.4) the packing of clusters becomes looser and hence the opacity of the aerogel increases [32, 33].

The contact angle increased continuously with the increase of  $M$  from 0.09 to 0.9 (as shown in Fig. 5). At lower  $M$  due to insufficient HMDZ, the incomplete surface modification occurs and hence the contact angle is less. The contact angle increased with the increase

of  $M$  due to an increase in the hydrophobicity of the aerogels. The contact angle is measured with respect to water. A water drop placed on the aerogel surface will be characterized by a contact angle ( $\theta$ ), if the difference between the solid-liquid and liquid-vapour interfacial energy is greater than zero. The balance of the phases is given by the Young's equation [34, 35].

$$\gamma_{sv} = \gamma_{sl} + \gamma_{lv}(\cos \theta) \quad (10)$$

Based on the Young's equation one would expect that only one value of contact angle for a particular solid/liquid drop/gas system should appear. The contact angle depends on the surface roughness, microscopic chemical heterogeneity, drop size, molecular re-orientation [36] and penetration of the liquid molecules into the solid surface. The surface hydroxyl groups are responsible for the hydrophilic nature of the aerogels [37–39]. During surface modification the  $-\text{H}$  groups are replaced by  $-\text{Si}(\text{CH}_3)_3$  groups resulting in dehydroxylation of the aerogel surface leading to hydrophobicity. This process drastically changes the physical as well as the chemical properties of the surface bulk of the aerogel.

Fig. 6 shows the FTIR spectra of the aerogels with the variation of  $M$ . The investigations indicate that the  $-\text{OH}$  bond peaks at 1600 and 3500  $\text{cm}^{-1}$  decreased with increase of  $M$  and these bands completely disappeared for  $M > 0.36$ . There are additional absorption bands at 2900, 2980, 1450  $\text{cm}^{-1}$  related to  $\text{C}-\text{H}$  bonds [40, 41], 2968 and 840  $\text{cm}^{-1}$  related  $\text{Si}-\text{C}$  of surface modified gels [42–44] and the intensity of these bands increased with increase of  $M$  from 0.09 to 0.9 indicating an increase in the surface modification. These facts reflect in the contact angles as shown in Fig. 5. Each monomer of HMDZ consists of two alkylsilane

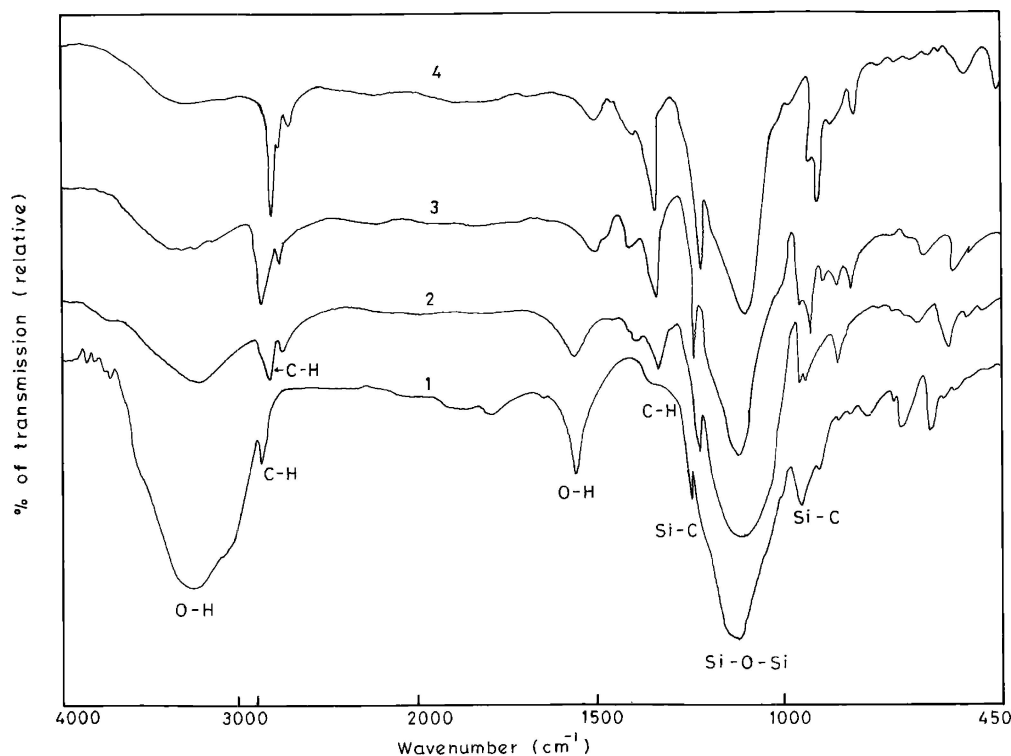


Figure 6 Infra red spectra of the aerogels with the variation of the HMDZ/TEOS ( $M$ ) molar ratio. 1 = 0.09, 2 = 0.18, 3 = 0.36, and 4 = 0.72 of  $M$ .

TABLE I

S. No	Molar ratio (A)	% of volume shrinkage	Density (gm/cm <sup>3</sup> )	% of porosity	Pore volume (cm <sup>3</sup> /gm)	Thermal conductivity (W/mK)
1	$3.115 \times 10^{-5}$	34	0.145	92.30	6.37	0.110
2	$6.23 \times 10^{-5}$	14	0.09	95.20	10.58	0.102
3	$3.115 \times 10^{-4}$	17	0.11	94.20	8.56	0.118
4	$6.23 \times 10^{-4}$	21	0.13	93.15	7.16	0.125
	(B)					
5	$4 \times 10^{-3}$	45	0.162	91.47	5.65	0.135
6	$8 \times 10^{-3}$	15	0.125	93.40	7.47	0.108
7	$4 \times 10^{-2}$	14	0.090	95.20	10.58	0.102
8	$8 \times 10^{-2}$	38	0.158	91.70	5.80	0.120
	(Wa)					
9	2	43	0.170	91.05	5.36	0.115
10	3.75	14	0.095	95.00	10.00	0.105
11	6.25	37	0.139	92.62	6.67	0.125
12	9	43	0.173	90.89	5.25	0.140
	(Wb)					
13	1.25	40.25	0.168	91.15	5.43	0.130
14	2.25	14.1	0.092	96.15	10.34	0.103
15	3.75	46.7	0.165	91.30	5.53	0.145
16	5.0	51.1	0.182	90.42	4.97	0.153

groups which get attached to the aerogel surface as described in Equation 8 [43]. Therefore with an increase of  $M$ , the number of alkyl groups attached to the surface of the aerogel increases, and hence the hydrophobicity of the surface also increases as observed from the increased intensity of the Si–C absorption band in the FTIR spectra. Hence the contact angle increases with increase of  $M$  values.

### 3.3. (Oxalic acid or NH<sub>4</sub>OH)/TEOS molar ratio

The aerogels were prepared with the variation of the molar ratios of oxalic acid/TEOS ( $A$ ) and NH<sub>4</sub>OH/TEOS ( $B$ ) from  $3.115 \times 10^{-5}$  to  $3.115 \times 10^{-3}$  and  $4 \times 10^{-3}$  to  $8 \times 10^{-2}$  respectively by keeping the molar ratio of TEOS:EtOH:acidicH<sub>2</sub>O:basicH<sub>2</sub>O:HMDZ constant at 1:8:3.75:2.25:0.36 respectively.  $B$  and  $A$  values were kept constant at  $4 \times 10^{-2}$  and  $6.23 \times 10^{-5}$  respectively while varying the  $A$  and  $B$ . The % of volume shrinkage, density and thermal conductivity of the aerogels decreased with the increase of  $A$  to  $6.23 \times 10^{-5}$  and  $B$  to  $4 \times 10^{-2}$  and then increased for  $A > 6.23 \times 10^{-5}$  and  $B > 4 \times 10^{-2}$  and whereas the % of porosity and pore volume increased with increase of  $A$  to  $6.23 \times 10^{-5}$  and  $B$  to  $4 \times 10^{-2}$  and then decreased for  $A > 6.23 \times 10^{-5}$  and  $B > 4 \times 10^{-2}$  of  $B$  as shown in Table. I. At lower  $A$  ( $< 6.23 \times 10^{-5}$ ) and  $B$  ( $< 4 \times 10^{-2}$ ) due to insufficient oxalic acid and ammonium hydroxide, the hydrolysis of TEOS, does not occur completely and condensation occurred among the hydrolysed –OH and unhydrolysed –OC<sub>2</sub>H<sub>5</sub> end groups to form the silica network, as shown in Equation 7, therefore nonuniform silica network formation is observed. Hence during drying, the shrinkage is more leading to the dense, with less % of porosity, high thermal conductivity aerogels. At higher  $A$  ( $> 6.23 \times 10^{-5}$ ) and  $B$  ( $> 4 \times 10^{-2}$ ) the presence of more oxalic acid and ammonium hydroxide resulted in faster hydrolysis and condensation of TEOS leading to fewer particle and pore sizes and therefore resulted in more shrunk, dense

and high thermal conductive and cracked aerogels [45]. Whereas, at  $A \approx 6.23 \times 10^{-5}$  and  $B \approx 4 \times 10^{-2}$ , complete hydrolysis and condensation of TEOS with uniform silica network occurred and particle and pore sizes also increased and hence the connectivity of the particles increased [46]. Hence, the aerogels with less shrinkage, low density, high pore volume high % of porosity and low thermal conductivity were obtained for  $A$  of  $6.23 \times 10^{-5}$  and  $B$  of  $4 \times 10^{-2}$  respectively.

The contact angle increased with increase of  $A$  to  $6.23 \times 10^{-5}$  and  $B$  to  $4 \times 10^{-2}$  and remained constant for  $A > 6.23 \times 10^{-5}$  and decreased for  $B > 4 \times 10^{-2}$  as shown in the Figs 7 and 8 respectively. At lower  $A$  and  $B$  due to incomplete hydrolysis of TEOS and condensation reactions, incomplete surface modification resulted. Hence, the entire surface of the silica network would not be hydrophobic. For  $A > 6.23 \times 10^{-5}$  there is no change in the contact angle because complete surface modification of silica network occurred whereas, the contact angle decreased for  $B > 4 \times 10^{-2}$  because of big particle sizes, less surface undergoes surface modification.

The transparency of the gels increased with increase of  $A$  to  $6.23 \times 10^{-5}$  and  $B$  to  $4 \times 10^{-2}$  and remained

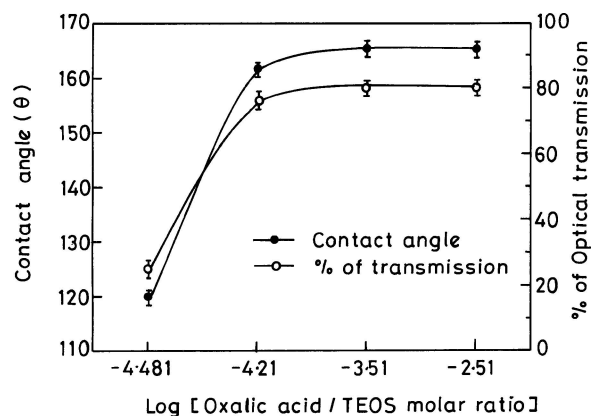


Figure 7 Change in the contact angle and % of optical transmission of the aerogels with the variation of the OXA/TEOS molar ratio ( $A$ ).

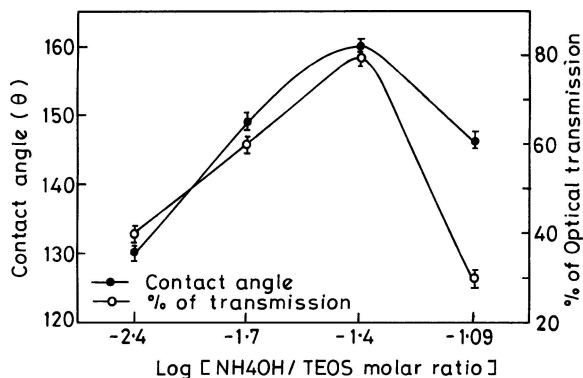


Figure 8 Change in the contact angle and % of optical transmission of the aerogels with the variation of the NH<sub>4</sub>OH/TEOS molar ratio (B).

constant for  $A > 6.23 \times 10^{-5}$  and decreased for  $B > 4 \times 10^{-2}$  as shown in Figs 7 and 8 respectively. This is because with increase of A and B to  $6.23 \times 10^{-5}$  and  $4 \times 10^{-2}$  respectively, particle and pore size growth is uniform so the transparency of the aerogels increased, where as at higher B values ( $>4 \times 10^{-2}$ ) due to fast condensation, cluster formation and irregular network structure forms leading to decrease in the optical transparency of the aerogels. Transparent aerogels were obtained for A and B values of  $6.23 \times 10^{-5}$  and  $4 \times 10^{-2}$  respectively.

### 3.4. Acidic or basic H<sub>2</sub>O/TEOS molar ratio

To study the effect of H<sub>2</sub>O/TEOS molar ratio on the physical properties of the aerogels, the acidic and basic H<sub>2</sub>O/TEOS molar ratios (Wa) and (Wb) varied from 2 to 9 and 1.25 to 5 respectively by keeping the TEOS:EtOH: OXA:NH<sub>4</sub>OH:HMDZ constant at 1:8:6.23 × 10<sup>-5</sup> :4 × 10<sup>-2</sup>:0.36 respectively. The values Wb and Wa were kept constant at 2.25 and 3.75 respectively for Wa and Wb variations. The % of volume shrinkage, density thermal conductivity decreased, pore volume and the % of porosity increased with the increase of Wa to 3.75 and Wb to 2.25 and the % of volume shrinkage, density, thermal conductivity increased for > 3.75 of Wa and > 2.25 of Wb as shown in the Table. I.

In the sol-gel process, H<sub>2</sub>O is used for hydrolysis and condensation reactions. An increase of Wa reduces the concentration of silicic acid per unit volume results in lower oxide content in the polymer product [47]. At low Wa, due to insufficient water for hydrolysis of TEOS, the silica net work surface contains unhydrolyzed -OC<sub>2</sub>H<sub>5</sub> groups. While condensation occurs among these groups resulting in dense gels. For Wa = 3.75 and Wb = 2.25 due to complete hydrolysis and condensation the modulus of the network increases due to more silica compared to Wa >3.75 and Wb >2.25 and hence, low density aerogels are obtained. Whereas in the case of high Wa and Wb (>3.75 and >2.25), the density is higher because water separates the silanol molecules and hinders the cross linking of the silane chain formation. Hence, during drying the gel shrunk more leading to dense aerogels. And also due to excess water, polymerization is lower than the hydrolysis

producing cyclization and enhancing the siloxane bond formation with in the particles resulted in packing of these densified particles into silica cluster formation.

With the increase of Wa to 3.75 and Wb to 2.25, shrinkage of the gels decreases and % of porosity increases and hence the thermal conductivity decreases. Further increase of Wa > 3.75 and Wb > 2.25, the thermal conductivity of the aerogels increases because the shrinkage increases and % of porosity decreases as shown in the Table. I.

The changes in the % of optical transmission and contact angle with the variation of Wa and Wb are shown in Figs 9 and 10 respectively. The contact angle and % of optical transmission increased with increase of Wa and Wb to 3.75 and remained constant for further increase of Wa > 3.75 whereas the contact angle remained constant and the % of optical transmission decreased for Wb > 3.75. At lower Wa and Wb, due to insufficient amount of water, the TEOS is not completely hydrolysed and therefore less number of silica clusters are formed. Since the silyl groups get attached to the silica clusters, the total silylation is less and therefore the contact angle is less leading to hydrophilic aerogels. On the other hand, increase of Wa and Wb leads to complete hydrolysis and condensation and thus more surface modification occurs, resulting in aerogels with higher hydrophobicity and therefore higher contact angle.

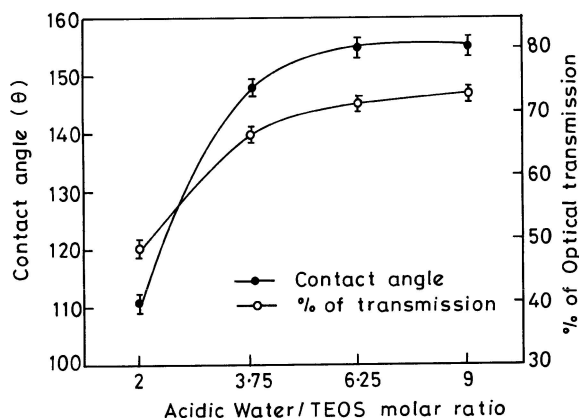


Figure 9 Change in the contact angle and % of optical transmission of the aerogels with the variation of the acidic H<sub>2</sub>O/TEOS molar ratio (Wa).

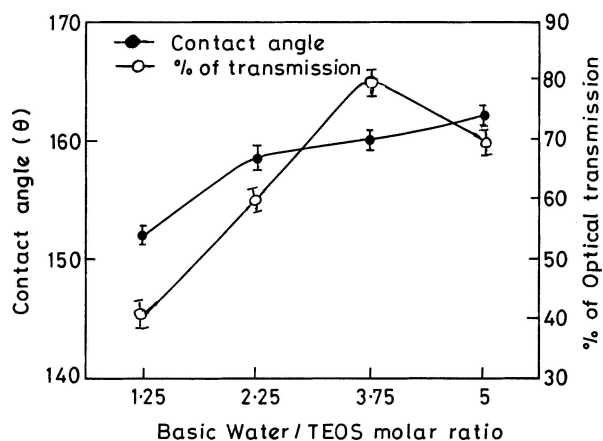


Figure 10 Change in the contact angle and % of optical transmission of the aerogels with the variation of the basic H<sub>2</sub>O/TEOS molar ratio (Wb).

At lower  $W_a$  ( $<3.75$ ) and  $W_b$  ( $<2.25$ ), the obtained aerogels were dense and translucent due to condensation of hydrolysed -OH and nonhydrolysed  $-OC_2H_5$  causing irregular growth of the particles and silica network leading to decrease in % of optical transmission. For  $W_a = 3.75$  and  $W_b = 2.25$ , uniform and regular growth of small silica particles and pore sizes were observed leading to homogeneous silica network, and hence the % of optical transmission increased as shown in the Figs 9 and 10. Whereas for  $W_b > 3.75$ , due to larger particle sizes, the % of optical transmission decreased as shown in the Fig. 10. Highly transparent, low density and low thermal conductive aerogels have been obtained for  $W_a$  and  $W_b$  values of 3.75 and 2.25 respectively.

### 3.5. EtOH/TEOS molar ratio (S)

Silica aerogels were prepared by varying the molar ratio of EtOH/TEOS ( $S$ ) from 1 to 16 by keeping the TEOS:acidic $H_2O$ :basic $H_2O$ :OXA: $NH_4OH$ :HMDZ constant at  $1:3.75:2.25:6.23 \times 10^{-5}:4 \times 10^{-2}:0.36$  respectively. The change in the % of volume shrinkage and density are shown in Fig. 11. It was observed that the % of volume shrinkage and density decreased with increase of  $S$  to 8 and then increased for  $S > 8$ . Ethanol solvent acts as a diluting agent which is very important in hydrolysis and condensation processes of the sol-gel method. For lower  $S$  ( $<8$ ), the % of volume shrinkage is more and cracked aerogels obtained because at lower  $S$ , the water content is more as compared to the higher  $S$ , cluster formation occur and therefore dense aerogels were obtained. For  $S > 8$ , in the presence of more solvent the oxide content per unit area in the hydrolysed product is less [47] and the particle separation is more which leads to cluster formation with less cross-linkages. During the drying process more shrinkage occurs and therefore dense aerogels obtained.

The % of porosity increased with the increase of  $S$  to 8 and then decreased for  $S > 8$  and hence the thermal conductivity decreased for  $S$  of 8 and increased for  $S > 8$  as shown in the Fig. 12. At lower and higher

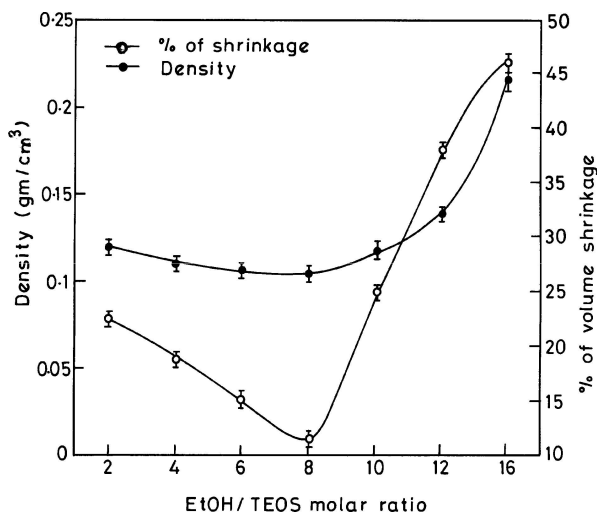


Figure 11 Change in the % of volume shrinkage and density of the aerogels with the variation of the EtOH/TEOS molar ratio ( $S$ ).

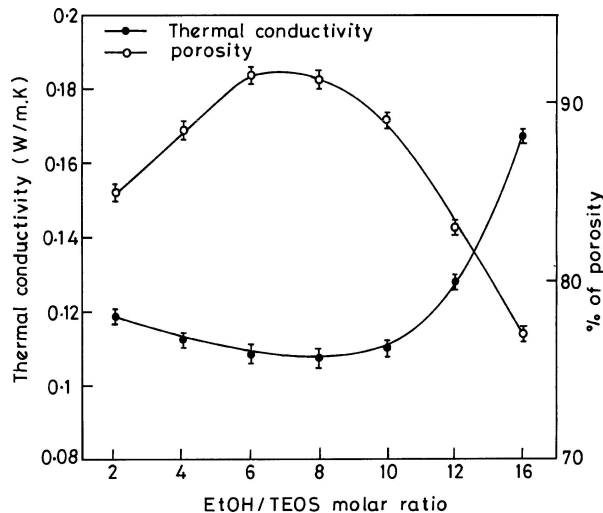


Figure 12 Change in the thermal conductivity and % of porosity of the aerogels with the variation of the EtOH/TEOS molar ratio ( $S$ ).

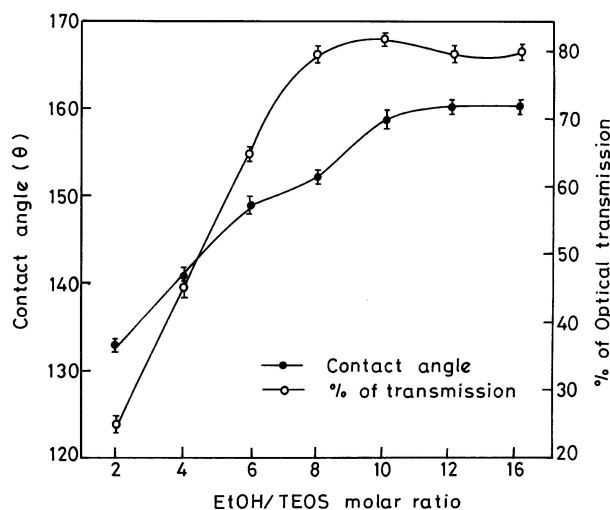


Figure 13 Change in the contact angle and % of optical transmission of the aerogels with the variation of the EtOH/TEOS molar ratio ( $S$ ).

$S$ , the aerogels shrunk more and hence the % of porosity is less and the thermal conductivity is high. The % of optical transmission and the contact angle of the aerogels increased with an increase of  $S$  up to 8 and remained constant for  $S > 8$  as shown in the Fig. 13. For  $S < 8$ , due to insufficient solvent, hydrolysis and condensation reactions occur slowly leading to inhomogeneity, irregular pore and particle size distribution and incomplete surface modification in the silica aerogel network which causes less % of optical transmission and low hydrophobicity to the aerogels. With the increase of  $S$  ( $>8$ ) due to complete hydrolysis and condensation of TEOS, which leads to uniform pore and particle sizes and complete surface modification resulting in transparent and hydrophobic aerogels. The contact angle also increased with the increase of  $S$  up to 8 and then remained constant for  $S > 8$  as shown in Fig. 13. Once the surface modification took place completely for  $S \approx 8$ , further increase of  $S$  ( $>8$ ) did not have any effect on the hydrophobicity of the aerogels. Transparent, hydrophobic low density and low thermal conductive silica aerogels were obtained with  $S$  value of 8.



#### 4. Conclusions

The obtained results show that the surface modification and the sol-gel parameters have great influencing effect on the physical properties of the ambient pressure dried silica aerogels. The molar ratios of sol-gel parameters such as HMDZ/TEOS (M), OXA/TEOS (A) NH<sub>4</sub>OH/TEOS (B), acidic H<sub>2</sub>O/TEOS (Wa), basic H<sub>2</sub>O/TEOS (Wb), EtOH/TEOS (S) were varied from 0.09 to 0.9,  $3.115 \times 10^{-5}$  to  $3.115 \times 10^{-3}$ ,  $4 \times 10^{-3}$  to  $8 \times 10^{-2}$ , 2 to 9, 1.25 to 5 and 1 to 16 respectively. During drying, the spring back effect was observed. The physical properties of the aerogels such as % of volume shrinkage, density and thermal conductivity, % of porosity, pore volume, % of optical transmission and contact angles were measured. In the FTIR spectra of the aerogels, it was found that the bands at 3500 and 1600 cm<sup>-1</sup> related to H-OH, Si-OH respectively decreased and the bands at 840 and 1250 cm<sup>-1</sup> of Si-C and 2900 and 1450 cm<sup>-1</sup> of C-H increased with increase of M. The best quality silica aerogels in terms of low density (0.075 gm/cm<sup>3</sup>), high porosity (96.5%) low thermal conductivity (0.090 W/mK), high hydrophobicity ( $\approx 160^\circ$ ) and high optical transmission (>90%) have been obtained with the molar ratio of TEOS:EtOH:acidicH<sub>2</sub>O:basicH<sub>2</sub>O:OXA:NH<sub>4</sub>OH:HMDZ at 1:8:3.75:2.25:6.23x10<sup>-5</sup>:4x10<sup>-2</sup>:0.36 respectively at ambient pressure dried method.

#### Acknowledgements

The authors gratefully acknowledge the funding for the present work from the Department of Science and Technology (DST), Government of India, New Delhi, under the project No SP/S2/CMP-01. The author Mrs. A. Parvathy Rao is highly thankful to the DST for the Research Associateship.

#### References

1. R. N. WENZEL, *J. Phys. Colloid. Chem.* **1466** (1949) 53.
2. A. B. D. CASSIE, *Faraday Soc.* **11** (1948) 3.
3. L. W. HRUBESH, *Chemistry and Industry* **124** (1990) 824.
4. J. FRICKE, "Aerogels" (Springer Verlag, Berlin, 1986)
5. R. J. AYEN and P. A. IACA BULA, *Rev. Chem. Eng.* **5** (1988) 157.
6. H. SCHNEIDER and A. BAIKER, *Catal. Rev. Sci. Eng.* **37** (1995) 513.
7. J. FRICKE and R. CAPS, "Ultra Structure Processing of Advanced Ceramic Materials" edited by J. D. Mackenzie and D. R. Ulrich (Wiley, New York, 1988) p. 613.
8. N. C. HOLMES, H. B. RADOUSKY, M. J. MOSS, W. J. NELLIS and S. HENNING, *Appl. Phys. Lett.* **45**(6) (1984) 626.
9. P. J. CARLSON, K. E. JOHANSSON, J. K. NORRBY, O. PINGOT, S. TAVENIER, F. VAN DEN BOGERT and L. VAN LANCKER, *Nucl. Instrum. Meth.* **160** (1979) 407.
10. J. PINTO DA CUNHA, F. NEVES and M. I. LOPES, *Nucl. Instrum. Meth. Phys. Res. A* **452** (2000) 401.
11. K. KIM, K. Y. JANG and R. S. UPADHYE, *J. Am. Ceram. Soc.* **74** (1991) 1987.
12. S. J. REED, C. S. ASHLEY, C. J. BRINKER, R. J. WALKO, R. ELLEFRON and J. GILL, *SPIE* **1328** (1990) 220.
13. G. M. PAJONK and S. J. TEICHNER, in Proceedings of the First International Symposium on Aerogels, edited

by J. Fricke (Wurzberg, Germany 23–25 September 1985) p. 193.

14. L. W. HRUBESH, report UCRL-21234, LLNL Livermore USA 1989.
15. R. CAPS and J. FRICKE, *Sol-Energy* **26** (1986) 361.
16. G. HARANATH, P. B. WAGH, G. M. PAJONK and A. VENKATESWARA RAO, *Mat. Res. Bull.* **32** (1997) 1079.
17. G. M. PAJONK, *Appl. Catal.* **72** (1991) 217.
18. K. SALLOUN, *J. Ele. Chem. Soc.* **142** (1995) 194.
19. D. M. SMITH, C. L. CLAVES, P. J. DAVIS and C. J. BRINKER, "Better Ceramics Through Chemistry," edited by C. J. Brinker, D. E. Clark and D. R. Ulrich, Mat. Res. Soc. Proc. 121, (Pitts Burgh, PA 1998) p. 657.
20. S. S. PRAKASH, C. J. BRINKER, A. J. HURD and S. M. RAO, *Nature* **374** (1995) 439.
21. A. VENKATESWARA RAO, E. NILSEN and M.-A. EINARSRUD, *J. Non-Cryst. Solids* **296** (2001) 165.
22. P. B. WAGH, R. BEGAG, G. M. PAJONK, A. VENKATESWARA RAO and D. HARANATH, *Mater. Chem. Phys.* **57** (1999) 224.
23. S. M. KIM, K. CHAKRABARTI, E. O. OH and C. M. WHANG, *J. Sol-Gel Sci. Technol.* **27** (2003) 149.
24. P. WAWZZYNAIL, G. ROGACKI, J. PRUBA and Z. BARTZAK, *J. Non-Cryst. Solids* **225** (2001) 50.
25. E. NILSEN, M.-A. EINARSRUD and G. W. SCHERER, *ibid.* **221** (1997) 135.
26. "Monsanto Santocel Product Literature Ad 166" (Monsanto Corp., St. Louis, MO 1959).
27. G. W. SCHERER, *J. Non-Cryst. Solids* **109** (1989) 183.
28. T. WOIGNER, J. PHALIPPOU and R. VACHER, *J. Mater. Res.* **4** (1989) 688.
29. G. W. SCHERER, D. M. SMITH X. XIU and J. ANDERSON, *J. Non-Cryst. Solids* **186** (1995) 316.
30. A. VENKATESWARA RAO, G. M. PAJONK, N. N. PARVATHY and E. ELALOUIE, in "Sol-Gel Processing and Applications" edited by Y.A. Attia (Plenum Publishing Company, New York, 1994) p. 237.
31. G. W. SCHERER, S. H. HAEREID E. NILSEN and M.-A. EINARSRUD, *J. Non-Cryst. Solids* **202** (1996) 42.
32. A. VENKATESWARA RAO, M. M. KULKARNI, G. M. PAJONK, D. P. AMALNERKAR and T. SETH, *J. Sol-Gel Sci. Technol.* **27** (2003) 103.
33. A. J. HUNT, *J. Non-Cryst. Solids* **225** (1998) 303.
34. A. W. ADAMAN, "Physical Chemistry of Surfaces" (John Wiley, New York, 1982) p. 338.
35. C. J. VANNOSS, R. F. GIESE and W. WU, *J. Dispers. Sci. Technol.* **19** (1998) 1221.
36. H. Y. ERBIL, G. MC. HALE, S. M. ROWAN and M. I. NEUTON, *Langmuir* **15** (1993) 73.
37. A. DASILVA, P. DONASO and M. A. AEGERTER *J. Non-Cryst. Solids* **145** (1992) 168.
38. L. J. BELLAMY, "The Infrared of Complex Molecule" (Wiley, New York, 1975).
39. N. HERING, K. SCHRIEBER, R. REIDER, O. LICHTENBERGER and J. WOLTERSODORF, *App. Organomet. Chem.* **15** (2001) 879.
40. C. J. Pouchert (ed) "Aldrich Library of FTIR Spectra (Aldrich Chemical, Wisconsin, 1985) Vol. 2.
41. M. LACZKA, K. CHOLEWA-KOWALSKA and M. KOGUL, *J. Non-Cryst. Solids* **287** (2001) 10.
42. A. E. YOUNG, *J. Sol-Gel Technol.* **19** (2000) 483.
43. H. YOKOGAWA and M. YOKOYAMA, *J. Non-Cryst. Solids* **186** (1995) 23.
44. K. H. LELE. S. Y. KIM and K. P. YOO, *ibid.* **186** (1995) 18.
45. C. J. BRINKER, *ibid.* **100** (1988) 31.
46. C. J. BRINKER and G. W. SCHERER, "Sol-Gel Science" (Academic press, Sandiego, 1990) p. 536.
47. B. E. YOLDAS, *J. Non-Cryst. Solids* **82** (1986) 11.

Received 7 September 2004  
and accepted 18 January 2005